DEPARTMENT OF DEFENCE

DEFENCE SCIENCE AND TECHNOLOGY ORGANISATION

AERONAUTICAL RESEARCH LABORATORIES

MELBOURNE, VICTORIA

MATERIALS NOTE 121

APPLICATION OF COMPLIANCE TECHNIQUES FOR STUDYING THE EFFECT OF SIDE-GROOVING ON STRESS-CORROSION CRACK KINETICS OF A HIGH STRENGTH STEEL

by

W. J. POLLOCK

Approved for Public Release

COPY No 10

April, 1978

AR-001-262

DEPARTMENT OF DEFENCE
DEFENCE SCIENCE AND TECHNOLOGY ORGANISATION
AERONAUTICAL RESEARCH LABORATORIES

(14) ARL/MAT-72

(9) MATERIALS NOTE 121

APPLICATION OF COMPLIANCE TECHNIQUES FOR STUDYING THE EFFECT OF SIDE-GROOVING ON STRESS-CORROSION CRACK KINETICS OF A HIGH STRENGTH STEEL

(10) by
W. J. POLLOCK

(11) Apr 77

(12) 24 p.

SUMMARY

Sub-critical crack growth was estimated from changes in compliance measured during the stress-corrosion cracking of D6AC steel at constant load using 1-T wedge-opening-loading specimens. Agreement of calculated mean crack growth with mean values measured from the fracture surface showed that plastic yielding at the crack tip during loading and subsequent stress-corrosion cracking was negligible. The analysis was then applied to side-grooved specimens where it was demonstrated that, under plane-strain conditions, side-grooving does not significantly affect the stress-corrosion cracking rate in D6AC steel.

POSTAL ADDRESS: Chief Superintendent, Aeronautical Research Laboratories,
Box 4331, P.O., Melbourne, Victoria, 3001, Australia.

CONTENTS

	Page No.
1. INTRODUCTION	1
2. THEORY	1
2.1 Specimen with no Side-Grooves	1
2.2 Specimen with Side-Grooves	1–2
2.3 Estimation of Crack-Growth from Compliance Measurements during Stress-Corrosion Cracking	2
3. EXPERIMENTAL	2–3
4. RESULTS AND DISCUSSION	3–4
5. CONCLUSIONS	4
REFERENCES	
TABLES	
FIGURES	
DISTRIBUTION	

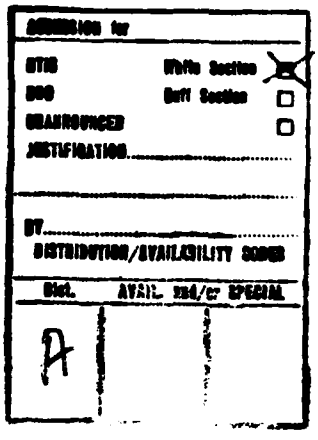

1. INTRODUCTION

Although compliance measurements are often used in fracture toughness and stress-corrosion testing to estimate stress intensities[1-8], they are employed less frequently to calculate sub-critical crack growth[5-8]. Difficulties which arise in estimating crack growth from compliance measurements include[9] (a) non-linear changes in compliance per unit crack growth with increasing crack length (with the exception of tapered double cantilever beam specimens), (b) extremely small changes in compliance with increase in crack length (e.g. centre-cracked specimens), and (c) time-dependent plasticity effects at the crack tip; this effect is manifested by an increase in compliance during loading (due to non-linearity of the crack-opening-displacement v load curve) and may also occur during subsequent stress-corrosion, especially if the stress intensity is increasing during cracking. Compliance changes produced by yielding and crack growth would then be indistinguishable. These yielding effects would be most noticeable at high loads and in low-strength alloys. The present work shows how the significance of the last effect was checked by measuring the change in compliance during the stress-corrosion cracking of a 1-T wedge-opening-loading (WOL) specimen and comparing the calculated crack growth with direct measurements on the fracture surface. For D6AC steel, these plasticity effects were insignificant and the compliance method was then used to study the effects of side-grooving on the compliance and stress-corrosion crack-growth rates in distilled water.

2. THEORY

2.1 Specimen with no Side-Grooves

A stress analysis and experimental confirmation of this analysis for the 1-T WOL specimen have been documented by Novak and Rolfe[10]. The plane-strain stress intensity K_{ungr} of a specimen with no side-grooves is given by[10]:

$$K_{ungr} = PC_3/(Ba^{\frac{1}{2}}) \quad [1]$$

where P is the load, B is the specimen thickness and C_3 is a function of the crack length a and the specimen depth W and is given by:

$$C_3 = [30{\cdot}96(a/W) - 195{\cdot}8(a/W)^2 + 730{\cdot}6(a/W)^3 - 1186{\cdot}3(a/W)^4 + 754{\cdot}6(a/W)^5] \quad [2]$$

The plane-strain stress intensity function is normally expressed as a function of the rate of change of compliance with crack length, $(dc/da)_{ungr}$, according to the relation [11-12]:

$$K_{ungr} = (G_{ungr}\,E/(1-\nu^2))^{\frac{1}{2}} = P[E/(2B(1-\nu^2))]^{\frac{1}{2}}(dc/da)^{\frac{1}{2}}_{ungr} \quad [3]$$

where G_{ungr} is the crack extension force, E is Young's modulus and ν is Poisson's ratio. Combining equations 3 and 1 gives:

$$(dc/da)_{ungr} = 2(1-\nu^2)\,C_3^2/(BaE) \quad [4]$$

2.2 Specimen with Side-Grooves

In the case of a specimen with side-grooves, it has been suggested that the acting stress intensity K_{gr} be modified according to the equation [13]:

$$K_{gr} = K_{ungr}\,(B/B_N)^m \quad [5]$$

where B_N is the reduced thickness across the crack front and m is an exponent which can have values in the range $0{\cdot}5 \leqslant m \leqslant 1{\cdot}0$. Previous experiments[13] have shown that m approaches $0{\cdot}5$ when the toughness in the cracking direction is low compared to the flank direction.

If equation 3 is now applied to a side-grooved specimen[11-12], then:

$$K_{gr} = (G_{gr}E/(1-\nu^2))^{\frac{1}{2}} = P(E/(2B_N(1-\nu^2)))^{\frac{1}{2}}(dc/da)^{\frac{1}{2}}_{gr} \quad [6]$$

where G_{gr} is the crack extension force and $(dc/da)_{gr}$ is the rate of change of compliance with crack length for the side-grooved specimen. Substituting equations 3 and 6 into equation 5 gives:

$$(dc/da)_{gr} = (dc/da)_{ungr}\,(B/B_N)^{2m-1} \quad [7]$$

$(dc/da)_{gr}$ can be expressed in terms of Novak and Rolfe's C_3 function by substituting equation 4 into equation 7:

$$(dc/da)_{gr} = [2(1-\nu^2)C_3^2/(BaE)](B/B_N)^{2m-1} \quad [8]$$

If $m = 0{\cdot}5$, then equation 7 shows that $(dc/da)_{gr} = (dc/da)_{ungr}$ and equations 1 and 5 indicate that $K_{gr} = PC_3/((BB_N)^{\frac{1}{2}}a^{\frac{1}{2}})$; this is the expression used by Novak and Rolfe in their studies using shallow side-grooved specimens ($B/B_N = 1{\cdot}1$). Correction factors for dc/da and K are given in figures 1 and 2 respectively for various m and B/B_N values. It is seen that these factors can be quite substantial except in cases where the side-grooves are shallow or values of m are close to $0{\cdot}5$.

2.3 Estimation of Crack-Growth from Compliance Measurements during Stress-Corrosion Cracking

Since contributions to compliance can arise from time-dependent plasticity effects at the crack tip during loading and subsequent stress-corrosion cracking, this possibility must be examined before reliable estimates of crack growth can be made. Information can be obtained by the following method, provided dc/da is known and the length of the crack before and after stress-corrosion cracking is measured. The latter information can be obtained by fatiguing the specimen before and after stress-corrosion cracking and measuring the crack lengths from the fracture surface after the specimen is broken open.

If a series of loads P_1, P_2, P_3, . . ., P_n are applied, then the following iterative procedure can be adopted to estimate the amount of stress-crorosion crack growth at each load level. For stress-corrosion cracking at load P_1, the initial crack length a_1 is known. An approximate value for the final crack length (a_2) is estimated and this estimate improved until the measured rate of change of compliance with crack length during stress-corrosion cracking, $(\Delta COD/P_1)/(a_2 - a_1)$, agrees with dc/da at a mean crack length $(a_1 + a_2)/2$, where ΔCOD is the change in crack-opening-displacement at the load line during stress-corrosion cracking. The best estimate for a_2 now becomes the initial crack length for the second burst of stress-corrosion cracking at load P_2 and the procedure repeated. If the total calculated crack length (a_{n+1}) after stress-corrosion cracking at load P_n agrees with that measured from the fracture surface, then it appears likely that changes in compliance due to yielding at the crack tip are minimal.

The method can be further checked by inserting fatigue markers after each burst of stress-corrosion at constant load. In this case, however, since the initial and final crack lengths (a_1 and a_2 respectively) associated with each burst of crack propagation at constant load can be measured from the fracture surface, calculation of $(\Delta COD/P)/(a_2 - a_1)$ at a mean crack length of $(a_1 + a_2)/2$ can be compared directly with dc/da.

If changes in compliance during stress-corrosion cracking at constant load arise solely from changes in crack length, then this method can be extended to obtain experimental values for $(dc/da)_{gr}$ in side-grooved specimens. This method would then supplement the normal experimental procedure for obtaining dc/da values i.e. measurement of $\Delta COD/P$ over a range of crack lengths and subsequent differentiation of the resulting compliance v crack length curve.

3. EXPERIMENTAL

Experiments were conducted with 22·9 mm thick 1-T WOL specimens cut from the same batch of D6AC steel. Specimens were austenitised for 30 minutes at 930°C, quenched to 'Ausbay' at 520°C and held for 30 minutes, and either quenched into hot circulating oil at 60°C or salt-quenched to 210°C before cooling slowly to room temperature. Specimens were then double-tempered for 1 + 1 hours at 565°C. Composition, tensile and fracture toughness properties are listed in Table 1.

Specimens were machined with cracks aligned in the T–L orientation. Shallow side-grooves ($B_N = 20{\cdot}3$ mm) were machined in the specimens prior to heat treatment and deeper side-grooves

($B_N = 18{\cdot}0$ or $7{\cdot}9$ mm) were machined subsequently. The shallow side-groove had a radius of $1{\cdot}2$ mm whereas the deeper side-grooves were machined at an angle of 60° (fig. 3). Specimens were pre-cracked by fatigue at 10 Hz in air at 25°C and cracks extended to approximately 5 mm from the notch with the stress intensity varying from 2–20MPam$^{\frac{1}{2}}$.

Since it is often difficult to maintain cracking perpendicular to the direction of the applied load in ungrooved specimens, shallow side-grooved specimens ($B_N = 20{\cdot}3$ mm) were used to study if yielding at the crack tip contributed to changes in compliance during loading and subsequent stress-corrosion cracking as outlined in section 2.3. The deeper side-grooved specimens were used to obtain $(dc/da)_{gr}$ values from which a value of m could be calculated and crack-growth rates determined.

Specimens were stress-corroded at constant load in distilled water at 25°C using a cantilever beam rig and changes in COD were measured using a linear variable differential transducer (LVDT) placed on the top face of the specimen. All COD values obtained were converted to equivalent values at the load line using a method of similar triangles[10]. Unless otherwise stated, crack lengths were estimated from the fracture surface using the mean value of seven evenly spaced points ($B \rightarrow H$) across the width of the crack front (fig. 4).

4. RESULTS AND DISCUSSION

Shallow side-grooved specimens ($B/B_N = 1{\cdot}1$) were alternately stress-corroded in distilled water at constant load, dried and fatigued in air until fracture. Fig. 4 shows a typical fracture surface in which regions of stress-corrosion are clearly distinguished from those of fatigue. The mean rate of change of compliance with crack length for each region of stress-corrosion cracking is plotted as a function of mean crack length in figure 5 and compared with the results of Novak and Rolfe for $m = 0{\cdot}5$ (i.e. $(dc/da)_{ungr}$) and $m = 1$. It is seen that all the experimentally determined dc/da values lie within $\pm 10\%$ of Novak and Rolfe's results ($0{\cdot}5 < m < 1{\cdot}0$), therefore implying that long-term plasticity effects are insignificant during the stress-corrosion of D6AC steel. Mean crack-growth measurements can therefore be measured to within $\pm 10\%$ and stress intensities estimated to within $\pm 3\%$ since $K \propto (dc/da)^{\frac{1}{2}}$ (equations 3 and 6). The magnitude of the scatter precludes a realistic determination of the exponent m in equation 5.

The validity of this method for determining crack growth was also demonstrated in the case where a number of consecutively applied loads were used during stress-corrosion cracking. A shallow side-grooved specimen ($B/B_N = 1{\cdot}1$) was fatigue-precracked and stress-corroded for varying periods of time at seven different loads before fatiguing and breaking open the specimen. The total mean crack growth was measured from the fracture surface and found to be $5{\cdot}5$ mm. Knowing the total change in COD during stress-corrosion cracking at each load level, the crack-growth increment during each period of stress-corrosion at constant load was calculated, using $(dc/da)_{gr}$ values obtained from Novak and Rolfe with $m = 0{\cdot}5$, and the total of these increments was found to be $5{\cdot}7$ mm. A similar calculation using $(dc/da)_{gr}$ with $m = 1{\cdot}0$ gave a value of $5{\cdot}1$ mm. The error in this case was again less than 10% and confirmed that the method could be used to provide accurate estimates of crack growth.

An estimate of the exponent m in equation 5 was obtained using side-grooved 1-T WOL specimens with $B/B_N = 2{\cdot}9$. Figure 6 shows the fracture surface of such a specimen which had been alternately fatigued in air and stress-corroded at constant load in distilled water at 25°C. It is noted that side-grooving caused the crack front to lead at the specimen edges resulting in considerable bowing of the crack front. Values of $(\Delta COD/P)/(a_2 - a_1)$ (i.e. $(dc/da)_{gr}$) are plotted in figure 7 as a function of crack length for each increment of stress-corrosion cracking. Also shown in figure 7 are corresponding $(dc/da)_{gr}$ values deduced from experimentally determined compliance ($\Delta COD/P$) measurements taken before each increment of fatigue and stress-corrosion and which were subsequently differentiated with respect to crack length a. The good agreement between the two methods confirms the applicability of using stress-corrosion data for estimating dc/da values. Values of m were estimated from equation 7 and plotted as a function of crack length in figure 8. Due to crack curvature, values of $(dc/da)_{gr}$ and hence m will vary with the method used to measure the mean crack length. Figure 8 shows that m only remains constant with crack length provided the component of crack length at the edge of the specimen is ignored (i.e. 3 point mean and 7 point mean). Since there is no apparent reason why m should vary

with crack length, the best estimate of crack length would appear to be given by the 7 point mean and the corresponding value for m is therefore 0·70.

The effect of side-groove depth on stress-corrosion cracking rate in distilled water at 25°C was studied using both oil-quenched and salt-quenched D6AC specimens tempered to 565°C and with B/B_N values of 1·1, 1·5 and 2·9. As shown in figure 9, the difference in quenching rate (salt versus oil) does not affect the stress-corrosion cracking rate in shallow side-grooved specimens ($B/B_N = 1·1$). Moreover, the effect of machining deeper side-grooves ($B/B_N = 1·5$ and 2·9) in either of these heat-treated specimens does not alter the stress-corrosion crack-growth rate significantly.

Plane-strain conditions (viz. $B > 2·5(K^2/\sigma_{ys}^2))^9$ (σ_{ys} is the yield stress) prevail over the full range of sub-critical cracking shown in figure 9. Cracking is therefore controlled by the plane-strain conditions at the specimen centre even though shear lips ($\sim 5\%$ of total fracture surface area) are present during overload in the shallow-grooved specimens ($B/B_N = 1·1$). These shear lips are characteristic of plane-stress conditions prevailing close to the specimen edge and due to the insensitivity of these regions to stress-corrosion cracking[14], convex-shaped crack fronts often develop during sub-critical cracking. Application of deeper side-grooves removes these shear lips during overload suggesting that the last traces of plane stress near the specimen surface have been removed. The enhancement of concave-shaped crack fronts may be due to notching effects which could introduce a stress-concentration factor close to the surface. Although this stress-concentration factor may be sufficient to reverse the curvature of the crack front, the apparent insensitivity of side-grooving to stress-corrosion crack-growth rate confirms that cracking is controlled by the plane-strain regions remote from the specimen sides. It is therefore concluded that crack-front curvature is much more sensitive to side-grooving than crack-growth rate in circumstances where plane-strain conditions prevail. In thinner specimens, however, where a greater proportion of plane stress exists, side-grooving might be expected to have a more substantial effect on crack-growth rate since (a) the ratio of plane strain to plane stress would be substantially increased by side-grooving, and (b) stress-corrosion crack-growth rates under plane-strain conditions are several orders of magnitude greater than under plane-stress conditions[14].

5. CONCLUSIONS

Compliance measurements have been used to demonstrate that yielding at the crack tip during stress-corrosion cracking of ultra-high strength D6AC steel at room temperature is not important. It has also been shown that changes in compliance due to stress-corrosion cracking can be used to estimate both stress intensity and crack growth without recourse to conventional compliance measurements. Finally, under conditions of plane strain, side-grooving was found to affect crack curvature but not stress-corrosion crack rate.

REFERENCES

1. Standard E399-74, Am. Soc. Test. Mat., (1974).
2. J. D. Landes and R. P. Wei, Int. J. Fract. Mech. **9**, 277, (1973).
3. M. V. Hyatt, Report D6-24466, Boeing Co. (1969).
4. C. S. Carter, Metall. Trans. **1**, 1551, (1970).
5. W. A. Van der Sluys, Eng. Fract. Mech. **1**, 447, (1969).
6. S. R. Novak and S. T. Rolfe, Corros. **26**, 121, (1970).
7. C. S. Kortovich and E. A. Steigerwald, Eng. Fract. Mech. **4**, 637, (1972).
8. A. A. Sheinker and J. D. Wood, Stress-Corrosion Cracking of Metals-A State of the Art, ASTM STP 518, Am. Soc. Test Mat., 16, (1972).
9. B. F. Brown, Metall. Rev. **13**, 171, (1968).
10. S. R. Novak and S. T. Rolfe, J. Mater. **4**, 701 (1969).
11. G. R. Irwin and J. A. Kies, Weld. J. Res. Inst. **19**, 193, (1954).
12. G. R. Irwin, Fracture Mechanics, Structural Mechanics, Pergamon Press, Oxford, 557, (1960).
13. C. N. Freed and J. M. Krafft, J. Mater. **1**, 770, (1966).
14. W. W. Gerberich and Y. T. Chen, Scripta Metall. **8**, 243, (1974).

TABLE 1
Composition and Properties of D6AC Steel

	C	*Mn*	*Si*	*P*	*S*	*Cr*	*Ni*	*Mo*	*V*	*Fe*
Wt. %	0·45	0·75	0·22	0·004	0·005	1·10	0·67	1·00	0·090	remainder

Quench Medium	*UTS* (MPa)	K_{IC} (MPam$^{\frac{1}{2}}$)
oil	1590	94
salt	1600	90

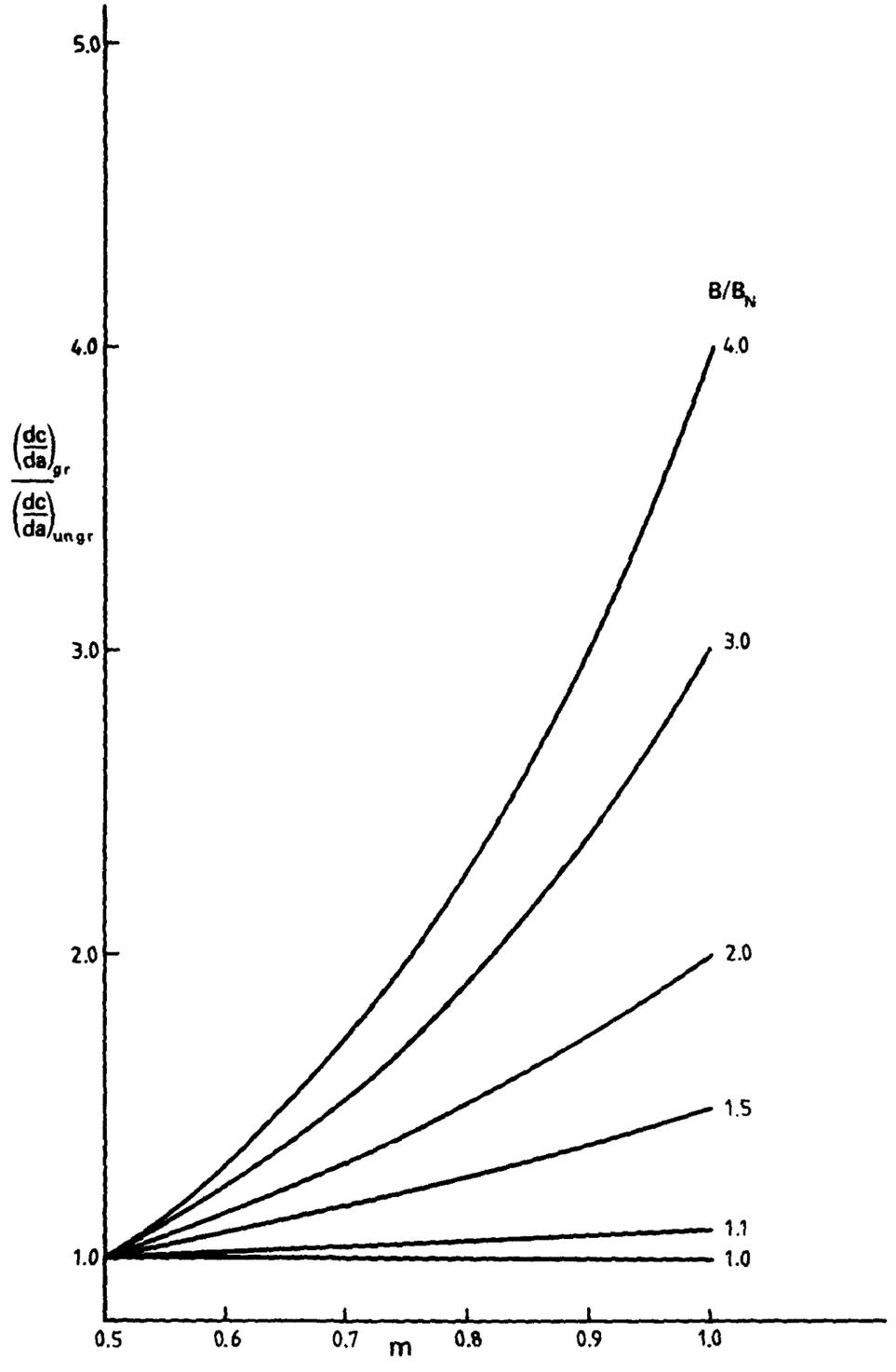

FIG. 1 VARIATION IN $\frac{dc}{da}$ WITH m FOR 1-T WOL SPECIMENS OF VARYING SIDE-GROOVE DEPTH

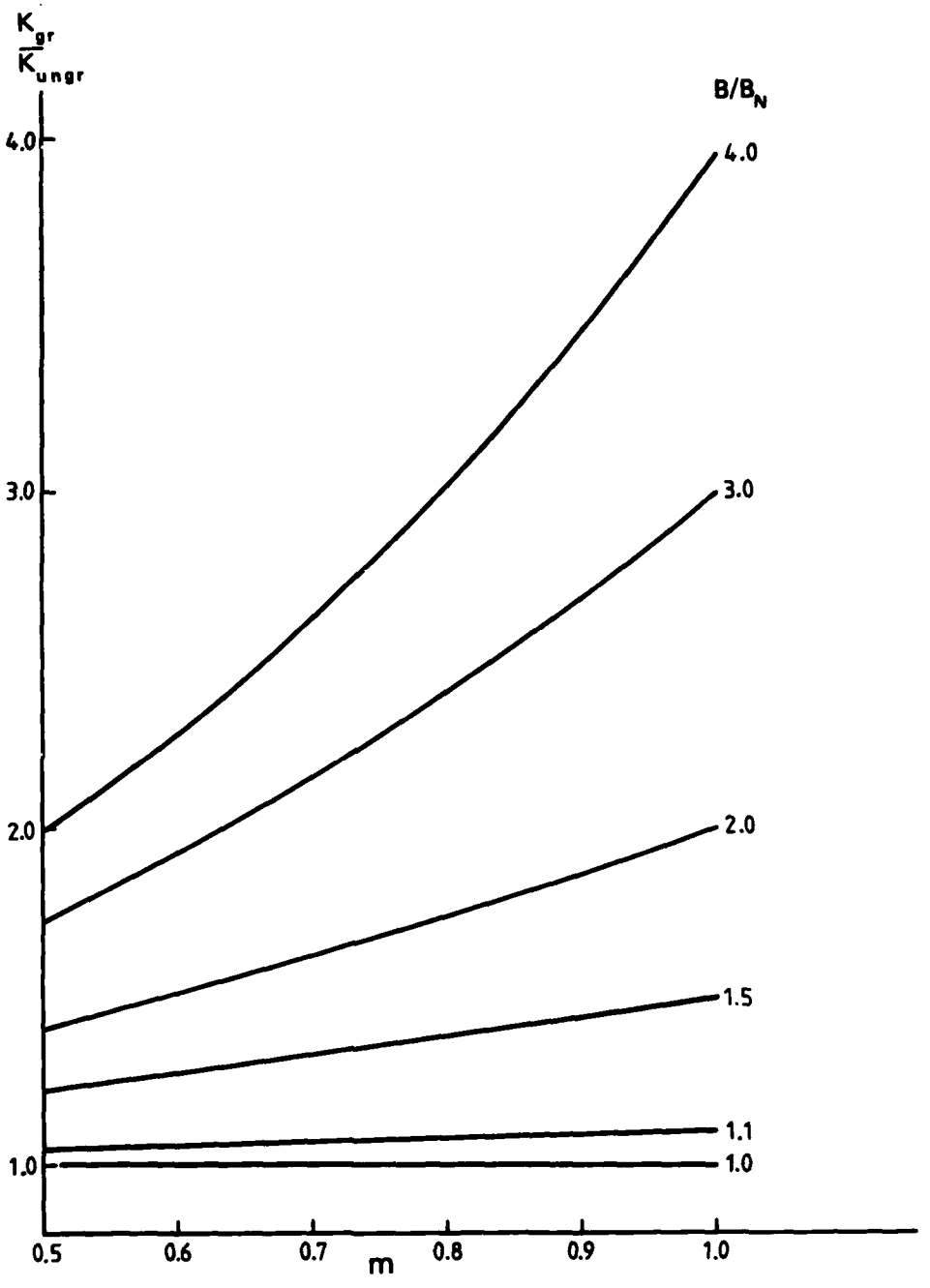

FIG. 2 VARIATION IN STRESS INTENSITY WITH m FOR 1-T WOL SPECIMENS OF VARYING SIDE – GROOVE DEPTH

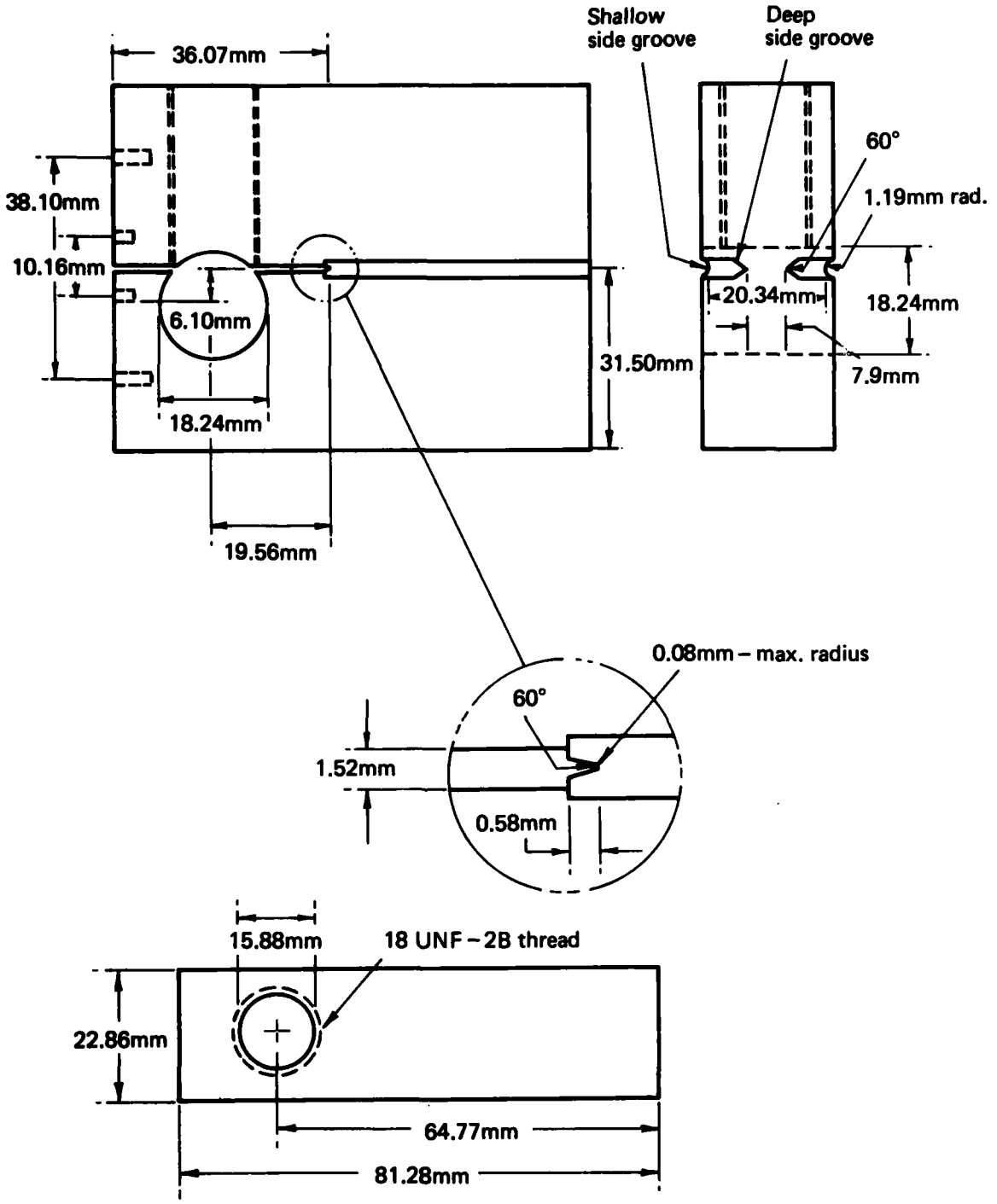

FIG. 3 MODIFIED 1-T WOL SPECIMEN

FIG. 4 FRACTURE SURFACE OF 1-T WOL SPECIMEN WITH B/B_N = 1.1 WHICH HAS BEEN ALTERNATELY FATIGUED AND STRESS-CORRODED

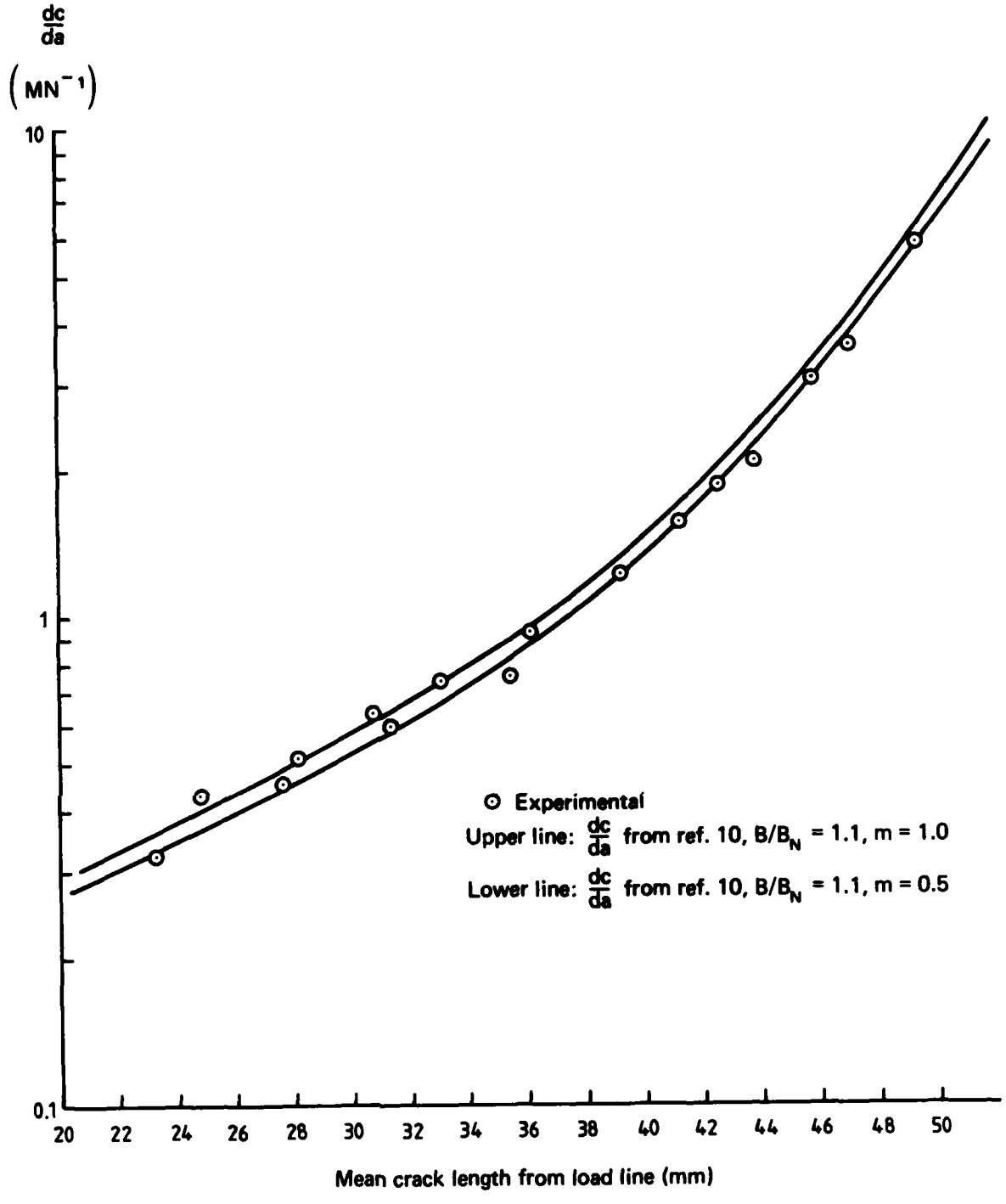

FIG. 5 EXPERIMENTAL $\frac{dc}{da}$ VALUES ESTIMATED FROM STRESS-CORROSION DATA

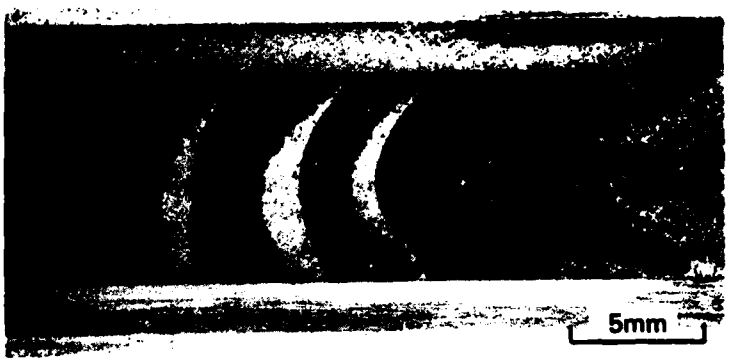

FIG. 6 FRACTURE SURFACE OF 1-T WOL SPECIMEN WITH B/B_N = 2.9 WHICH HAS BEEN ALTERNATELY FATIGUED AND STRESS-CORRODED

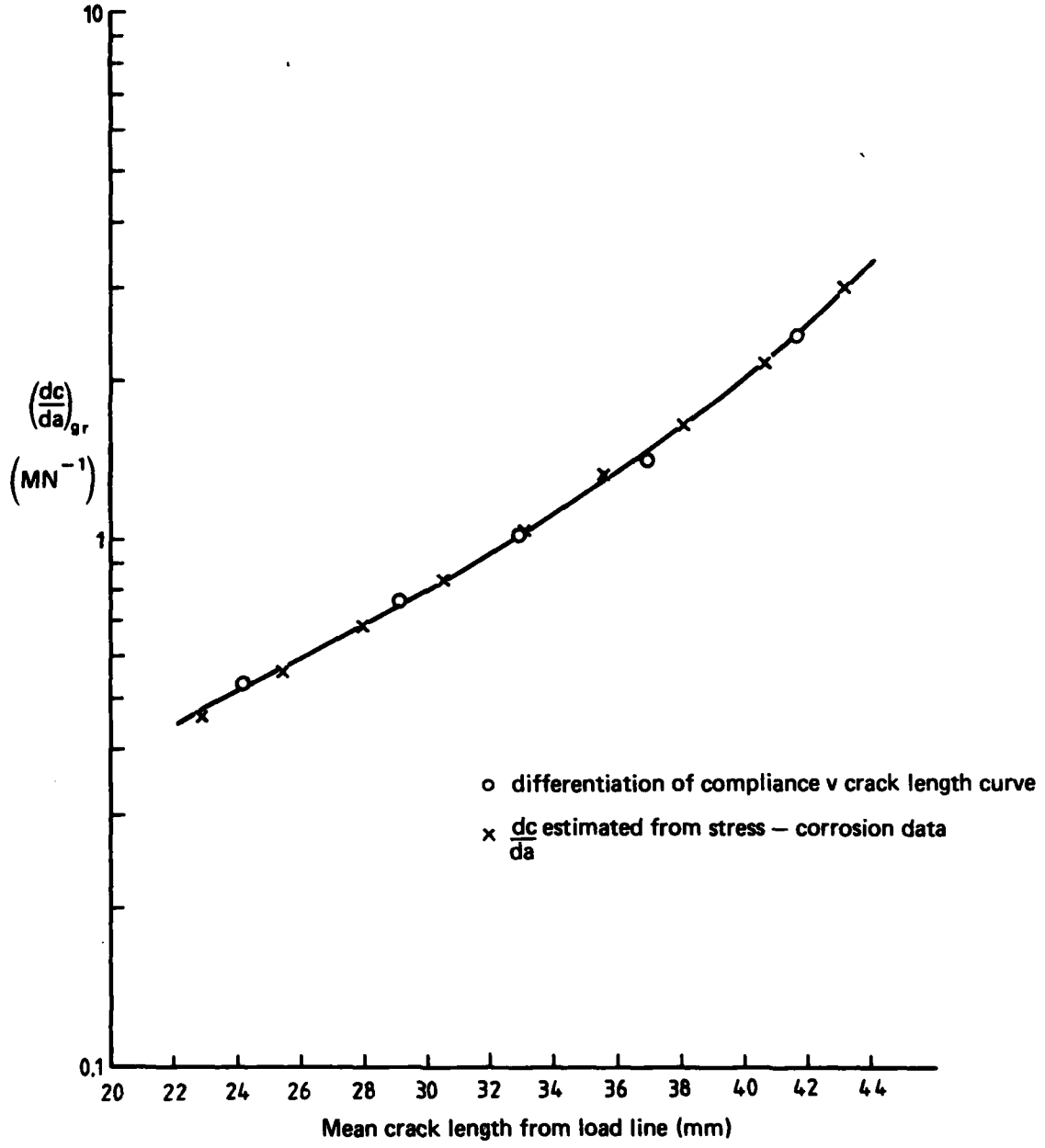

FIG. 7 $\left(\frac{dc}{da}\right)_{gr}$ VALUES FOR DEEP SIDE-GROOVED SPECIMEN (B/B_N = 2.9)

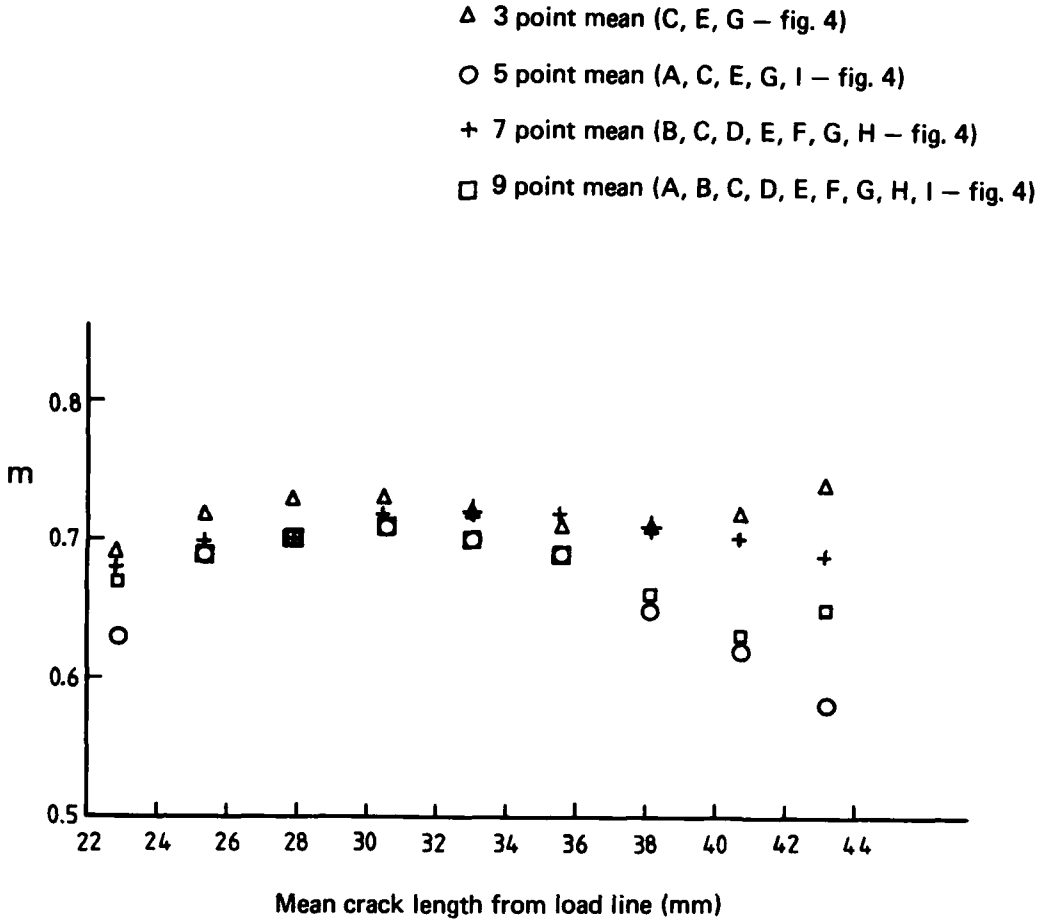

FIG. 8 VARIATION IN m WITH MEAN CRACK LENGTH

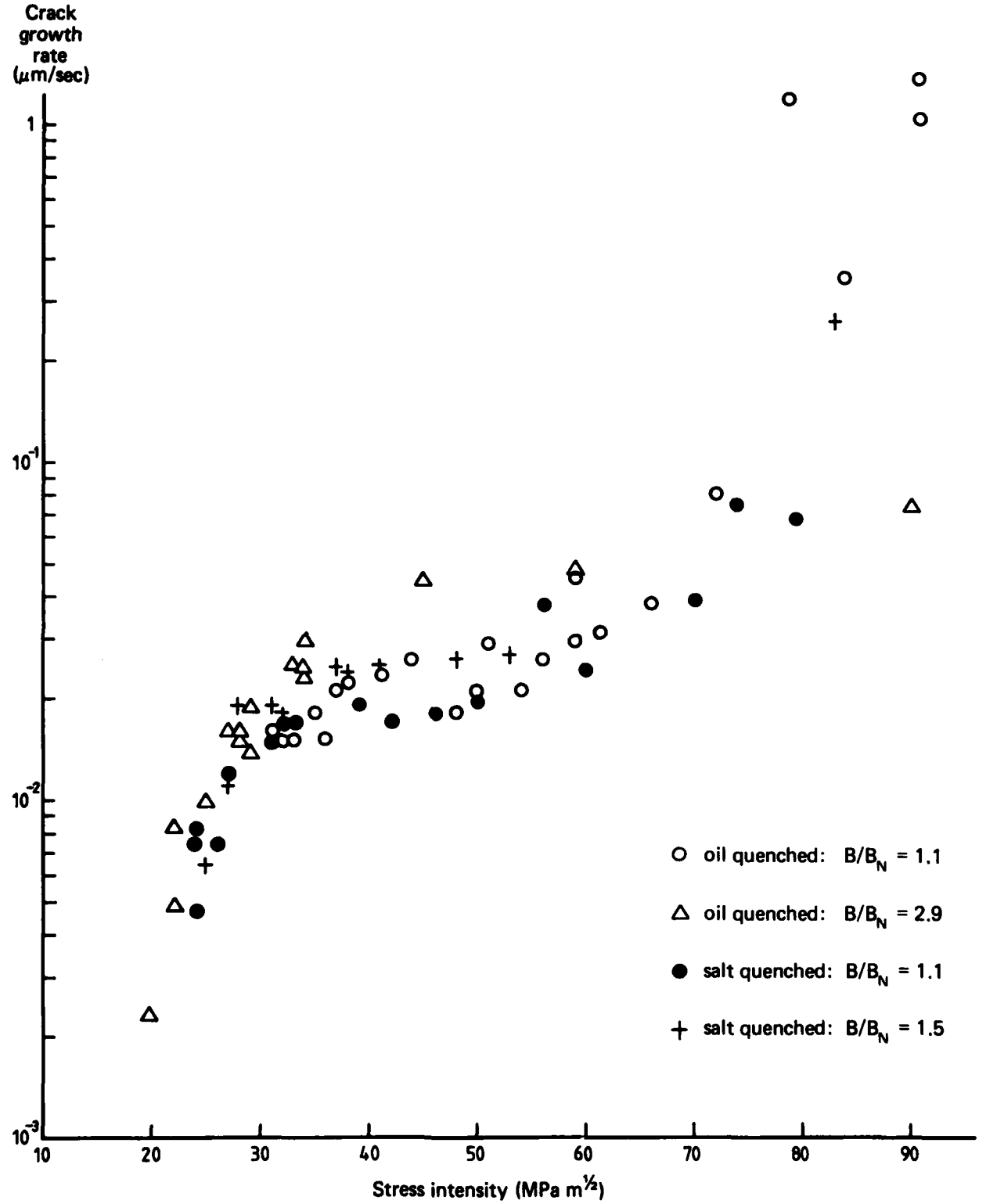

FIG. 9 EFFECT OF SIDE-GROOVING ON STRESS-CORROSION CRACK-GROWTH RATE

DOCUMENT CONTROL DATA SHEET

Security classification of this page Unclassified

1. Document Numbers
   (a) AR Number: AR-001-262
   (b) Document Series and Number: Materials-Note-121
   (c) Report Number: ARL-Mat-Note-121

2. Security Classification
   (a) Complete document: Unclassified
   (b) Title in isolation: Unclassified
   (c) Summary in isolation: Unclassified

3. Title: APPLICATION OF COMPLIANCE TECHNIQUES FOR STUDYING THE EFFECT OF SIDE-GROOVING ON STRESS-CORROSION CRACK KINETICS OF A HIGH STRENGTH STEEL

4. Personal Author(s): W. J. Pollock

5. Document Date: April, 1978

6. Type of Report and Period Covered:

7. Corporate Author(s):

8. Reference Numbers
   (a) Task: DST 76/93
   (b) Sponsoring Agency:

9. Cost Code: 35 4745

10. Imprint: Aeronautical Research Laboratories, Melbourne

11. Computer Program(s) (Title(s) and language(s)): N.A.

12. Release Limitations (of the document) Approved for Public Release

12-0. Overseas:	No.		P.R.	1	A		B		C		D		E	

13. Announcement Limitations (of the information on this page): No Limitation

14. Descriptors:
Crack propagation
Modulus of elasticity
Stress corrosion
Cracking (Fracturing)
High strength steels
D6AC Steel
Side grooving

15. Cosati Codes:
1113
2012

16.

ABSTRACT

Sub-critical crack growth was estimated from changes in compliance measured during the stress-corrosion cracking of D6AC steel at constant load using 1-T wedge-opening-loading specimens. Agreement of calculated mean crack growth with mean values measured from the fracture surface showed that plastic yielding at the crack tip during loading and subsequent stress-corrosion cracking was negligible. The analysis was then applied to side-grooved specimens where it was demonstrated that, under plane-strain conditions, side-grooving does not significantly affect the stress-corrosion cracking rate in D6AC steel.

DISTRIBUTION

	Copy No.
AUSTRALIA	
DEPARTMENT OF DEFENCE	
Central Office	
Chief Defence Scientist	1
Executive Controller, ADSS	2
Superintendent, Defence Science Administration	3
Defence Library	4
JIO	5
Assistant Secretary, DISB	6–21
Aeronautical Research Laboratories	
Chief Superintendent	22
Superintendent, Materials Division	23
Divisional File, Materials Division	24
Author: W. J. Pollock	25
Library	26
Materials Research Laboratories	
Library	27
Defence Research Centre	
Library	28
Engineering Development Establishment	
Library	29
RAN Research Laboratory	
Library	30
Navy Office	
Naval Scientific Office	31
Army Office	
Army Scientific Adviser	32
Royal Military College	33
US Army Standardisation Group	34
Air Force Office	
Air Force Scientific Adviser	35
Engineering (CAFTS) Library	36
D. Air Eng.	37
H.Q. Support Command (SENGSO)	38
DEPARTMENT OF PRODUCTIVITY	
Australian Government Engine Works (Mr J. L. Kerin)	39
Government Aircraft Factories, Library	40
DEPARTMENT OF TRANSPORT	
Director-General/Library	41
Airworthiness Group (Mr R. Ferrari)	42

STATUTORY, STATE AUTHORITIES AND INDUSTRY

Australian Atomic Energy Commission (Director)		43
CSIRO Central Library		44
CSIRO Mechanical Engineering Division (Chief)		45
CSIRO Tribophysics Division (Director)		46
Qantas, Library		47
Trans Australia Airlines, Library		48
Ministry of Fuel and Power (Secretary) Victoria		49
SEC Herman Research Laboratory, Librarian, Vic.		50
Ansett Airlines of Australia, Library		51
BHP Central Research Laboratories, NSW		52
BHP Melbourne Research Laboratories		53
Commonwealth Aircraft Corporation (Manager)		54
Commonwealth Aircraft Corporation (Manager of Engineering)		55
Hawker de Havilland Pty. Ltd. (Librarian) Bankstown		56
Hawker de Havilland Pty. Ltd. (Manager) Lidcombe		57
ICI Australia Ltd. Library		58

UNIVERSITIES AND COLLEGES

Adelaide	Barr Smith Library	59
	Professor of Mechanical Engineering	60
Australian National	Library	61
Flinders	Library	62
James Cook	Library	63
La Trobe	Library	64
Melbourne	Engineering Library	65
Monash	Library	66
	Professor I. J. Polmear, Mat. Eng.	67
Newcastle	Library	68
New England	Library	69
New South Wales	Physical Sciences Library	70
	Professor R. A. A. Bryant, Mech. and Ind. Eng.	71
	Assoc. Professor R. W. Traill-Nash, Struc. Eng.	72
	Professor P. T. Fink, Mech. and Ind. Eng.	73
	Professor A. H. Willis, Mech. and Ind. Eng.	74
Queensland	Library	75
Sydney	Professor G. A. Bird, Aero. Eng.	76
	Professor J. W. Roderick, Mech. Eng.	77
	Professor R. I. Tanner, Mech. Eng.	78
Tasmania	Engineering Library	79
	Professor A. R. Oliver, Civil and Mech. Eng.	80
Western Australia	Library	81
	Professor Allen-Williams, Mech. Eng.	82
RMIT	Library	83
	Mr Millicer, Aero. Eng.	84
	Mr Pugh, Mech. Eng.	85

CANADA

CAARC Co-ordinator, Structures	86
NRC, National Aeronautics Establishment, Library	87

UNIVERSITIES

McGill Library	88
Toronto Institute of Aerophysics	89

FRANCE

AGARD, Library	90
ONERA, Library	91
Service de Documentation, Technique de l'Aeronautique	92

INDIA

CAARC Co-ordinator Materials 93
CAARC Co-ordinator Structures 94
Civil Aviation Department (Director) 95
Defence Ministry, Aero. Development Establishment, Library 96
Hindustan Aeronautics Ltd. Library 97
Indian Institute of Science, Library 98
Indian Institute of Technology 99
National Aeronautical Laboratory (Director) 100

ISRAEL

Technion—Israel Institute of Technology 101

ITALY

Associazione Italiana di Aeronautica and Astronautica, (Professor A. Evla) 102

JAPAN

National Aerospace Laboratory, Library 103

UNIVERSITIES

Tohoku (Sendai) Library 104
Tokyo Institute of Space and Aerospace 105

NETHERLANDS

Central Organization for Applied Science Research in the Netherlands TNO, Library 106
National Aerospace Laboratory (NLR) Library 107

NEW ZEALAND

Air Dept. RNZAF, Aero. Documents Section 108
Transport Ministry, Civil Aviation Division, Library 109

UNIVERSITIES

Canterbury Library 110

SWEDEN

Aeronautical Research Institute 111

SWITZERLAND

Institute of Aerodynamics E.T.H. 112
Institute of Aerodynamics (Professor J. Ackeret) 113

UNITED KINGDOM

Australian Defence Science and Technical Representative 114
Aeronautical Research Council, NPL (Secretary) 115
CAARC, NPL (Secretary) 116
Royal Aircraft Establishment Library, Farnborough 117
Royal Aircraft Establishment Library, Bedford 118
Royal Armament Research and Development Est., Library 119
Aircraft and Armament Experimental Est. 120
Admiralty Materials Laboratories (Dr R. G. Watson) 121
National Engineering Laboratories (Superintendent) 122
National Physical Laboratories, Aero. Division (Superintendent) 123
British Library, Science Reference Library 124
British Library, Lending Division 125
Naval Construction Research Establishment (Superintendent) 126
CAARC Co-ordinator, Structures 127
Aircraft Research Association, Library 128
Fulmer Research Institute Ltd. (Research Director) 129
Metals Abstracts (Editor) 130
Rolls Royce (1971) Ltd., Aeronautics Division (Chief Librarian) 131

Rolls-Royce (1971) Ltd., Bristol Siddeley Division		132
Science Museum Library		133
Welding Institute, Library		134
Hawker Siddeley Aviation Ltd., Brough		135
Hawker Siddeley Aviation Ltd., Greengate		136
Hawker Siddeley Aviation Ltd., Kingston-upon-Thames		137
Hawker Siddeley Dynamics Ltd., Hatfield		138
British Aircraft Corporation (Holdings) Ltd., Commercial Aircraft Div.		139
British Aircraft Corporation (Holdings) Ltd., Military Aircraft		140
British Hovercraft Corporation Ltd., (E. Cowes)		141
UNIVERSITIES AND COLLEGES		
Cambridge	Library, Engineering Department	142
Nottingham	Library	143
Southampton	Library	144
Strathclyde	Library	145
Cranfield Institute of Technology	Library	146
Imperial College	The Head	147
UNITED STATES OF AMERICA		
Counsellor, Defence Science		148
NASA Scientific and Technical Information Facility		149
American Institute of Aeronautics and Astronautics		150
The Chemical Abstracts Service		151
Boeing Co. Head Office		152
Boeing Co. Industrial Production Division		153
General Electric (Aircraft Engine Group)		154
Lockheed Aircraft Co. (Director)		155
McDonnell Douglas Corporation (Director)		156
Westinghouse Laboratories (Director)		157
United Aircraft Corporation, Fluid Dynamics Labs.		158
United Aircraft Corporation, Pratt and Whitney Aircraft Div.		159
UNIVERSITIES AND COLLEGES		
California	Dr M. Holt, Department of Aerosciences	160
Cornell (New York)	Library, Aeronautical Laboratories	161
Florida	Mark H. Clarkson, Department of Aero. Eng.	162
Spares		163–172